Entropy of Transmitter Maps in Cooperative Multipath Assisted Positioning

Markus Ulmschneider, Christian Gentner and Armin Dammann
German Aerospace Center (DLR), Institute of Communications and Navigation
Muenchner Str. 20, 82334 Wessling, Germany
{markus.ulmschneider,christian.gentner,armin.dammann}@dlr.de

***Abstract*—In multipath assisted positioning, multipath components (MPCs) are regarded as line-of-sight (LoS) signals from virtual transmitters. The locations of physical and virtual transmitters are typically unknown, but can be estimated jointly with the location of a mobile terminal using simultaneous localization and mapping (SLAM). When users cooperate by exchanging maps of estimated positions of physical and virtual transmitters, the positioning performance can be improved drastically. Within this paper, we investigate such transmitter maps that are shared among users. We derive an approximation of the entropy of transmitter maps that is based on the unscented transform and analyze the evolution of this entropy over time. Our simulations indicate that the transmitter maps converge quickly.**

***Index Terms*—cooperative Channel-SLAM, cooperative positioning, entropy, maps, simultaneous localization and mapping**

I. Introduction

Multipath propagation has for a long time been regarded an inhibiting factor in wireless localization systems. Using standard algorithms based on the time of arrival (ToA) for example, multipath components (MPCs) tend to bias range estimates and therefore decrease the localization performance [1]. In particular in urban canyons and indoors, where much multipath propagation can be expected, this performance of wireless localization systems may be degraded crucially.

However, the spatial information contained in MPCs can be exploited for positioning. In multipath assisted positioning schemes, MPCs are regarded as line-of-sight (LoS) signals from *virtual transmitters*. The generic term transmitter may refer to either a virtual or physical transmitter in the following.

If the structure of the environment of a mobile terminal, e.g. from a detailed floor plan, and the location of the physical transmitter(s) are known, the locations of these virtual transmitters can be calculated in advance [2]–[4]. The physical transmitter could be a wireless local area network (WLAN) router or a base station from any other terrestrial signal of opportunity (SoO), for example.

In general, though, such information on the environment is not available. In this case, the location of the transmitters can be estimated jointly with the location of the mobile terminal [5]–[8] with simultaneous localization and mapping (SLAM). One such approach is Channel-SLAM [9], [10], which, in SLAM terms, simultaneously localizes a mobile terminal and maps transmitters. A resulting transmitter map contains posterior probability density functions (PDFs) that describe the estimated locations of transmitters. In the following, the term map will denote such a transmitter map.

We have previously extended the single user Channel-SLAM scheme to cooperative Channel-SLAM in [11], [12], where users cooperate by sharing maps. In a crowd-sourcing like scheme, multiple users going through the same scenario share and constantly improve maps. Maps can be improved by adding new transmitters to the map and by decreasing the variance of locations of transmitters that are already in the map with own observations. We have shown that cooperative Channel-SLAM outperforms the single user Channel-SLAM approach significantly [12].

The focus of this paper is an analysis of the maps that are shared in cooperative Channel-SLAM. In particular, we have a look at the evolution of the entropy of transmitter locations in maps. Since the single transmitter locations in a map are represented by particle clouds, a closed-form solution to calculate the entropy of a map does not exist. Hence, we derive an approximation based on sigma point methods. We evaluate the entropy of maps in cooperative Channel-SLAM based on simulations in an indoor scenario.

Regarding the notation, the term user may refer to a person or the radio receiver the person is equipped with, depending on the context. The variable c_0 denotes the speed of light. As indices, k refers to a time instant, i to a user particle, j to a transmitter, ℓ to a transmitter particle, and m to a sigma point. The Dirac delta distribution is denoted by $\delta(\cdot)$.

The remainder of the paper is organized as follows. Section II introduces cooperative Channel-SLAM. The concept of entropy and its application in maps are presented in Section III. Experimental results based on simulations in an indoor scenario are evaluated and discussed in Section IV. Finally, Section V concludes the paper.

II. Cooperative Channel-SLAM

A. Virtual Transmitters

Fig. 1 illustrates the idea of virtual transmitters. Neglecting the LoS signal for clarity, the transmit signal from the physical transmitter Tx arrives at the user via three different propagation paths.

Along the first propagation path drawn orange, the signal is reflected at a planar surface represented by the wall. The respective MPC is regarded by the user as a LoS signal from the virtual transmitter vTx1, which is located at the location

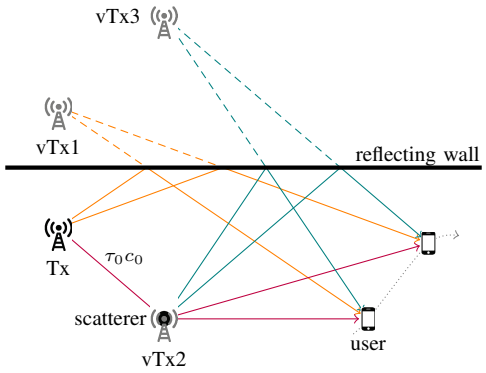

Fig. 1. The signal from the physical transmitter Tx arrives at the user via three different non-line-of-sight propagation paths as it interacts with the two objects in the environment. Each corresponding signal arriving at the user is regarded as a LoS signal from a virtual transmitter.

of Tx mirrored at the wall. Since the actual propagation path and the Euclidean distance between vTx1 and the user are the same, there is no time offset between Tx and vTx1.

Along the second propagation path drawn red, the signal is scattered by an object. In our model, we assume a perfect point scatterer that distributes the energy of the impinging signal uniformly to all directions. The signal arriving at the user is interpreted as a LoS signal from the virtual transmitter vTx2, located at the scatterer's location. In the case of the scattered signal, there is a delay offset τ_0 between Tx and vTx2, corresponding to the Euclidean distance $\tau_0 c_0$ between the two. A delay offset between a physical and a virtual transmitter can in general be interpreted as a clock offset.

The third propagation path drawn blue involves both the scatterer and the wall, leading to the virtual transmitter vTx3. It shows that the concept of single scattering and reflections can be extended to multiple interactions of the transmit signal with different objects. The virtual transmitter vTx3 is located at the scatterer's location mirrored at the wall, and has a delay offset τ_0 towards the physical transmitter Tx.

If the transmit signal interacts only with static planar surfaces and point scatterers, the locations of the virtual transmitters are static. Many other structures can be approximated sufficiently well by planar surfaces and scatterers, though.

B. Single User Channel-SLAM

We regard a mobile user in a static environment with only one physical transmitter Tx transmitting the signal $s(t)$. The linear multipath channel is time variant due to the movement of the user. The j^{th} signal component at time t is characterized by a complex amplitude $a_j(t)$ and a delay, or ToA, $\tau_j(t)$. The received signal is a sum of signal components,

$$y(\tau, t) = \sum_j a_j(t) s\left(\tau - \tau_j(t)\right) + n(\tau). \tag{1}$$

The term $n(\tau)$ describes colored noise incorporating both additive white Gaussian noise and dense multipath components (DMC). At the user, a snapshot of the received signal is sampled at time instants k, where we assume that the channel is constant for the length of one snapshot.

Channel-SLAM works in two stages. In the first stage, we use the Kalman Enhanced Super Resolution Tracking (KEST) [13] estimator to track the parameters of signal components over time with parallel Kalman filters. KEST uses the Space-Alternating Generalized Expectation-Maximization (SAGE) algorithm [14] for snapshot-wise channel estimation. The ToA and angle of arrival (AoA) estimates from the channel estimator at each time instant k are stacked in a vector $\boldsymbol{z}_k$.

In the second stage of Channel-SLAM, these estimates are used as measurements in a Rao-Blackwellized particle filter to estimate the state of the user and the states of the transmitters, as each signal component corresponds to one transmitter. The user state $\boldsymbol{x}_{\text{u},k}$ at time instant k is characterized by the user position $\boldsymbol{p}_{\text{u},k}$ and velocity $\boldsymbol{v}_{\text{u},k}$,

$$\boldsymbol{x}_{\text{u},k} = \left[\boldsymbol{p}_{\text{u},k}^T \;\; \boldsymbol{v}_{\text{u},k}^T\right]^T = \left[x_k \;\; y_k \;\; v_{x,k} \;\; v_{y,k}\right]^T. \tag{2}$$

The transmitters are assumed static in Channel-SLAM. The state $\boldsymbol{x}_{\text{TX},k}^{<j>}$ of the j^{th} transmitter at time instant k includes its location $\boldsymbol{p}_{\text{TX},k}^{<j>}$ and its clock offset $\tau_{0,k}^{<j>}$ multiplied by the speed of light,

$$\boldsymbol{x}_{\text{TX},k}^{<j>} = \left[\boldsymbol{p}_{\text{TX},k}^{<j>T} \;\; c_0\tau_{0,k}^{<j>}\right]^T = \left[x_{\text{TX},k}^{<j>} \;\; y_{\text{TX},k}^{<j>} \;\; c_0\tau_{0,k}^{<j>}\right]^T. \tag{3}$$

The overall state vector including the user state and the state of the $N_{\text{TX},k}$ transmitters, corresponding to the $N_{\text{TX},k}$ signal components detected by the channel estimator, is

$$\begin{aligned}\boldsymbol{x}_k &= \left[\boldsymbol{x}_{\text{u},k}^T \;\; \boldsymbol{x}_{\text{TX},k}^{<1>T} \;\; \dots \;\; \boldsymbol{x}_{\text{TX},k}^{<N_{\text{TX},k}>T}\right]^T \\ &= \left[\boldsymbol{x}_{\text{u},k}^T \;\; \boldsymbol{x}_{\text{TX},k}^T\right]^T.\end{aligned} \tag{4}$$

In Channel-SLAM, we estimate the history of this overall state $\boldsymbol{x}_{0:k}$ from time instants zero to k based on control inputs $\boldsymbol{u}_{1:k}$ and measurements $\boldsymbol{z}_{1:k}$, both from time time instants one to k. The control input may incorporate measurements from additional sensors, such as from an inertial measurement unit (IMU), for example. The state space is split into the user state and the transmitter space. The posterior PDF for the history of the state vector $\boldsymbol{x}_{0:k}$ from time instants zero to k is thus expressed as

$$\begin{aligned}\mathrm{p}\left(\boldsymbol{x}_{0:k}|\boldsymbol{z}_{1:k}, \boldsymbol{u}_{1:k}\right) &= \mathrm{p}\left(\boldsymbol{x}_{\text{TX},0:k}, \boldsymbol{x}_{\text{u},0:k}|\boldsymbol{z}_{1:k}, \boldsymbol{u}_{1:k}\right) \\ &= \mathrm{p}\left(\boldsymbol{x}_{\text{u},0:k}|\boldsymbol{z}_{1:k}, \boldsymbol{u}_{1:k}\right) \\ &\quad \times \mathrm{p}\left(\boldsymbol{x}_{\text{TX},0:k}|\boldsymbol{x}_{\text{u},0:k}, \boldsymbol{z}_{1:k}\right).\end{aligned} \tag{5}$$

The first factor in the second line of Eq. (5) is the posterior PDF of the user state. In the Rao-Blackwellized particle filter, it is represented by N_{p} samples in the state space, so called user particles, where the i^{th} user particle history $\boldsymbol{x}_{\text{u},0:k}^{<i>}$ is weighted by $w_{0:k}^{<i>}$. Hence we have for the user state

$$\mathrm{p}\left(\boldsymbol{x}_{\text{u},0:k}|\boldsymbol{z}_{1:k}, \boldsymbol{u}_{1:k}\right) = \sum_{i=1}^{N_{\text{p}}} w_{0:k}^{<i>} \delta\left(\boldsymbol{x}_{\text{u},0:k} - \boldsymbol{x}_{\text{u},0:k}^{<i>}\right). \tag{6}$$

In the Rao-Blackwellized particle filter, the states of the transmitters are estimated for each user particle independently

from the other particles. Following the uncorrelated scatterer assumption, the estimates from the channel estimator in the first stage are assumed to be uncorrelated for different transmitters. If some measurements are correlated, then only for a very short time. Hence, the posterior PDF of the history $\boldsymbol{x}_{\mathrm{TX},0:k}^{<i,j>}$ of the j^{th} transmitter's state conditioned on the i^{th} user particle from time instants zero to k is given by

$$\mathrm{p}\left(\boldsymbol{x}_{\mathrm{TX},0:k}^{<i>}|\boldsymbol{x}_{\mathrm{u},0:k}^{<i>},\boldsymbol{z}_{1:k}\right)=\prod_{j=1}^{N_{\mathrm{TX},k}}\mathrm{p}\left(\boldsymbol{x}_{\mathrm{TX},0:k}^{<i,j>}|\boldsymbol{x}_{\mathrm{u},0:k}^{<i>},\boldsymbol{z}_{1:k}\right). \quad (7)$$

The factors in the product on the right hand side of Eq. (7) are represented in the Rao-Blackwellized particle filter as a sum of particle histories, too. The ℓ^{th} of the $N_{\mathrm{p,Tx}}$ particles of the j^{th} transmitter and the i^{th} user particle is denoted by $\boldsymbol{x}_{\mathrm{TX},0:k}^{<i,j,\ell>}$, and its associated weight by $w_{0:k}^{<i,j,\ell>}$. The respective transmitter's posterior PDF is

$$\begin{aligned}&\mathrm{p}\left(\boldsymbol{x}_{\mathrm{TX},0:k}^{<i,j>}|\boldsymbol{x}_{\mathrm{u},0:k}^{<i>},\boldsymbol{z}_{1:k}\right)\\&\quad=\sum_{\ell=1}^{N_{\mathrm{p,Tx}}}w_{0:k}^{<i,j,\ell>}\delta\left(\boldsymbol{x}_{\mathrm{TX},0:k}^{<i,j>}-\boldsymbol{x}_{\mathrm{TX},0:k}^{<i,j,\ell>}\right).\end{aligned} \quad (8)$$

Note that the number of transmitter particles $N_{\mathrm{p,Tx}}$ may be different for different time instants, user particles and transmitters. Nevertheless, we omit the respective indices for notational brevity. A full derivation of single user Channel-SLAM can be found in [9].

C. Cooperative Channel-SLAM

In scenarios such as malls, museums or public buildings, multiple users roam in the same area on different trajectories. With Channel-SLAM, they estimate not only their own location, but also create maps of radio transmitter states in the environment. Such maps can be shared among users and used as prior information regarding the transmitter states in the scenario. Other users exploit this prior knowledge in the map and improve the map with own observations. We have shown previously that although the users are in different local coordinate systems, the positioning performance increases drastically with such a cooperative Channel-SLAM approach [12]. The estimation of the transformation parameters relating the coordinate system of the different users and establishing correspondences among transmitters observed by different users is denoted by the term map matching [15].

We define a comprehensive map created by a user in Channel-SLAM as the estimated states of transmitters marginalized over the user particles. The state $\boldsymbol{x}_{\mathrm{TX},k}^{<\cdot,j>}$ of the j^{th} transmitter in such a map is defined as

$$\begin{aligned}&\mathrm{p}\left(\boldsymbol{x}_{\mathrm{TX},k}^{<\cdot,j>}|\boldsymbol{z}_{1:k},\boldsymbol{x}_{\mathrm{u},0:k}\right)\\&\quad=\sum_{i=1}^{N_{\mathrm{p}}}w_k^{<i>}\sum_{\ell=1}^{N_{\mathrm{p,Tx}}}w_k^{<i,j,\ell>}\delta\left(\boldsymbol{x}_{\mathrm{TX},k}^{<\cdot,j>}-\boldsymbol{x}_{\mathrm{TX},k}^{<i,j,\ell>}\right).\end{aligned} \quad (9)$$

For each comprehensive map, the particles and weights are stored for each transmitter. Accordingly, the amount of data necessary to store a comprehensive map can be very high.

III. Entropy of Transmitter Maps

A. Transmitter State PDFs as Gaussian Mixture Models

To decrease the amount of data to be transmitted when sharing maps, we approximate the transmitter states' posterior PDFs in Eq. (9) with Gaussian mixture models [16]. The PDF of a Gaussian mixture model is represented by a set of weighted Gaussian distributions, also called components, where the weights sum up to one. This PDF for a random variable $\boldsymbol{x}$ is defined by

$$\mathrm{p}\left(\boldsymbol{x}\right)=\sum_{\ell=1}^{N_{\mathrm{C}}}w_\ell\mathcal{N}(\boldsymbol{x};\boldsymbol{\mu}_\ell,\boldsymbol{C}_\ell), \quad (10)$$

where $\mathcal{N}(\boldsymbol{x};\boldsymbol{\mu}_\ell,\boldsymbol{C}_\ell)$ is the ℓ^{th} of the N_{C} components, i.e., a Gaussian distribution with mean $\boldsymbol{\mu}_\ell$ and covariance matrix $\boldsymbol{C}_\ell$, with associated weight w_ℓ.

To estimate the parameters of the Gaussian mixture components that approximate the transmitter state PDFs as represented in Eq. (9), we use the Expectation-Maximization (EM) algorithm [17]. The number of components is determined with the Bayesian information criterion (BIC) [18].

B. Entropy of a Map

Following [19], we aim at finding a measure for the uncertainty of an estimated map. If the uncertainty about a map is low, the information content is high. One such measure is the differential entropy of a continuous random variable $\boldsymbol{x}$, which is defined as

$$h\left(\boldsymbol{x}\right)=-\int\mathrm{p}\left(\boldsymbol{x}\right)\log\left(\mathrm{p}\left(\boldsymbol{x}\right)\right)\mathrm{d}\boldsymbol{x}. \quad (11)$$

Compared to the covariance matrix, the entropy of a continuous random variable is a more adequate description of the information content for multi-modal distributions, in particular when the single modes are well separated.

A comprehensive map in cooperative Channel-SLAM consists of the posterior PDFs of the states of all transmitters in the map. The joint entropy of N independent random variables $\boldsymbol{x}_1,\ldots,\boldsymbol{x}_N$ is [20]

$$h\left(\boldsymbol{x}_1,\ldots,\boldsymbol{x}_N\right)=\sum_{j=1}^{N}h\left(\boldsymbol{x}_j\right). \quad (12)$$

Assuming independence among the transmitters in the map, the entropy of a comprehensive map is the sum of the entropies of the single transmitters.

Since there is no meaningful and closed-form solution to calculate the entropy for a particle cloud or a Gaussian mixture representation of a PDF, we will derive an approximation for the Gaussian mixture case in the following.

C. Approximation based on the Unscented Transform

To calculate the entropy of a Gaussian mixture model, we insert Eq. (10) into Eq. (11), yielding

$$\begin{aligned} & h\left(\boldsymbol{x}\right) \\ &= -\int \sum_{\ell=1}^{N_\mathrm{C}} w_\ell \mathcal{N}(\boldsymbol{x};\boldsymbol{\mu}_\ell,\boldsymbol{C}_\ell) \log\left(\sum_{\tilde{\ell}=1}^{N_\mathrm{C}} w_{\tilde{\ell}} \mathcal{N}\left(\boldsymbol{x};\boldsymbol{\mu}_{\tilde{\ell}},\boldsymbol{C}_{\tilde{\ell}}\right)\right) \mathrm{d}\boldsymbol{x} \\ &= -\sum_{\ell=1}^{N_\mathrm{C}} w_\ell \int \mathcal{N}(\boldsymbol{x};\boldsymbol{\mu}_\ell,\boldsymbol{C}_\ell) \log\left(\sum_{\tilde{\ell}=1}^{N_\mathrm{C}} w_{\tilde{\ell}} \mathcal{N}\left(\boldsymbol{x};\boldsymbol{\mu}_{\tilde{\ell}},\boldsymbol{C}_{\tilde{\ell}}\right)\right) \mathrm{d}\boldsymbol{x} \\ &= -\sum_{\ell=1}^{N_\mathrm{C}} w_\ell \int \mathcal{N}(\boldsymbol{x};\boldsymbol{\mu}_\ell,\boldsymbol{C}_\ell)\, \boldsymbol{g}\left(\boldsymbol{x}\right) \mathrm{d}\boldsymbol{x}, \end{aligned} \tag{13}$$

where we define the second factor in the integral of the third line as $\boldsymbol{g}\left(\boldsymbol{x}\right)$. Due to this non-linear function $\boldsymbol{g}\left(\boldsymbol{x}\right)$, the integral in the last line of Eq. (13) can not be calculated in closed form.

However, we can make use of the unscented transform, which allows to approximate this integral by propagating so called sigma points through the function $\boldsymbol{g}\left(\boldsymbol{x}\right)$. In general, an integral over the product of a Gaussian PDF $\mathcal{N}(\boldsymbol{x};\boldsymbol{\mu}_{\boldsymbol{x}},\boldsymbol{C}_{\boldsymbol{x}})$ and a function $\boldsymbol{g}\left(\boldsymbol{x}\right)$ can be approximated by [21]

$$\int \boldsymbol{g}(\boldsymbol{x}) \mathcal{N}(\boldsymbol{x};\boldsymbol{\mu}_{\boldsymbol{x}},\boldsymbol{C}_{\boldsymbol{x}})\, \mathrm{d}\boldsymbol{x} \approx \sum_{m=1}^{N_\mathrm{sig}} \omega_m \boldsymbol{g}(\boldsymbol{X}_m), \tag{14}$$

where the m^{th} of the N_sig sigma points is denoted by $\boldsymbol{X}_m$ and its associated weight by ω_m. In contrast to Monte Carlo (MC) methods, these point are not chosen randomly, but deterministically with the goal to preserve the original statistics of $\boldsymbol{x}$ when being propagated through a nonlinear function. There are several choices for the sigma points and their weights in the literature. For example, they are defined in [22] for some $\kappa \in \mathbb{R}$ as

$$\begin{aligned} \boldsymbol{X}_0 &= \boldsymbol{\mu}_{\boldsymbol{x}}, & \omega_0 &= \frac{\kappa}{\kappa+N}, \\ \boldsymbol{X}_m &= \boldsymbol{\mu}_{\boldsymbol{x}} + \left(\sqrt{(N+\kappa)\boldsymbol{C}_{\boldsymbol{x}}}\right)_m, & \omega_m &= \frac{1}{2(\kappa+N)}, \\ \boldsymbol{X}_{m+N} &= \boldsymbol{\mu}_{\boldsymbol{x}} - \left(\sqrt{(N+\kappa)\boldsymbol{C}_{\boldsymbol{x}}}\right)_m, & \omega_{m+N} &= \frac{1}{2(\kappa+N)}, \end{aligned} \tag{15}$$

leading to $2N+1$ sigma points for $m = 1, ..., N$. In Eq. (15), $(\boldsymbol{A})_m$ denotes the m^{th} row or column of the matrix $\boldsymbol{A}$, and

$$(N+\kappa)\boldsymbol{C}_{\boldsymbol{x}} = \sqrt{(N+\kappa)\boldsymbol{C}_{\boldsymbol{x}}} \sqrt{(N+\kappa)\boldsymbol{C}_{\boldsymbol{x}}}^T. \tag{16}$$

With Eq. (14), the entropy in Eq. (13) of one transmitter's state PDF is approximated by

$$h\left(\boldsymbol{x}\right) \approx -\sum_{\ell=1}^{N_\mathrm{C}} w_\ell \sum_{m=1}^{N_\mathrm{sig}} \omega_{\ell,m} \boldsymbol{g}(\boldsymbol{X}_{\ell,m}), \tag{17}$$

where $\boldsymbol{X}_{\ell,m}$ is the m^{th} sigma point corresponding to the ℓ^{th} component and $\omega_{\ell,m}$ its associated weight. The entropy of a comprehensive map can be calculated then with Eq. (12).

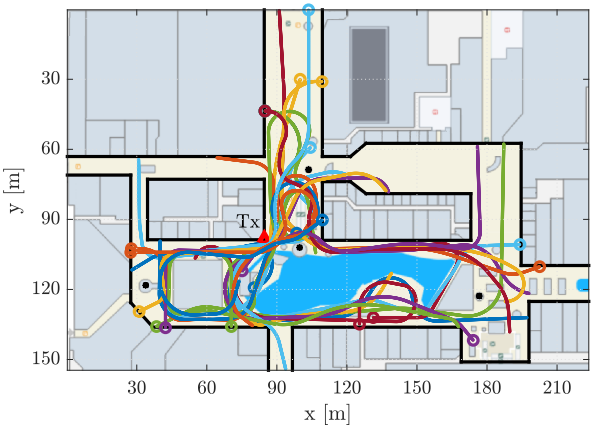

Fig. 2. Top view of the simulation scenario with 22 user tracks. There is one physical transmitter labeled Tx. The walls represented by black lines and the scatterers represented by the black dots reflect and scatter the transmit signal from Tx.

IV. Simulations

A. Simulation Scenario

While the concept of single user Channel-SLAM has been validated with real measurement data in [9], for example, we performed simulations in an indoor mall to evaluate our approach. A top view of the simulation scenario is depicted in Fig. 2. The red triangle labeled Tx represents the only physical transmitter. The reflecting walls represented by thick black lines and the point scatterers represented by the black dots create a multipath environment. There are 22 independent and random user tracks in the scenario typical for an indoor mall. The starting point of each track is marked by a circle.

The transmit signal is generic with a bandwidth of 100 MHz and a perfectly constant power spectral density around the carrier frequency of 1.9 GHz. The bandwidth is a crucial factor of multipath assisted positioning schemes, as they rely on the ability to resolve MPCs at the receiver. With a small bandwidth, the channel estimator may not be able to resolve arriving signal components, leading to undetected signal components and biased estimates as well as potentially false association decisions. Nevertheless, the signal bandwidth in this paper was chosen to be in the order of bandwidths used in currently used wireless communication systems. Angular change rates of the receiver are available from a gyroscope that is rigidly mounted to the receiver. These change rates are incorporated as control input in Channel-SLAM. Our channel model for the simulations is a AWGN channel neglecting DMC. In a real scenario, KEST can deal with DMC when it is handled in the snapshot-based estimator SAGE.

For each user position, we simulate the band-limited channel impulse response (CIR) based on the environment with ray-tracing. The users travel with a constant speed of 1 m/s. Every 100 ms, a snapshot of the received signal is recorded at the respective receiver and used for Channel-SLAM. We assume

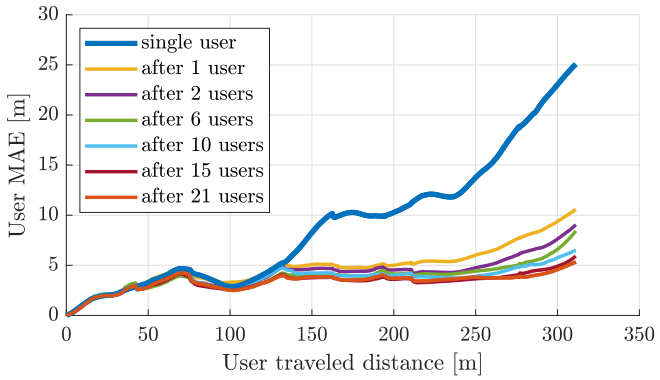

Fig. 3. MAE versus the distance traveled by the reference user with different prior knowledge. In the single user case, the reference user has no prior transmitter map. In the other cases, a number of user have contributed to the reference user's prior transmitter map.

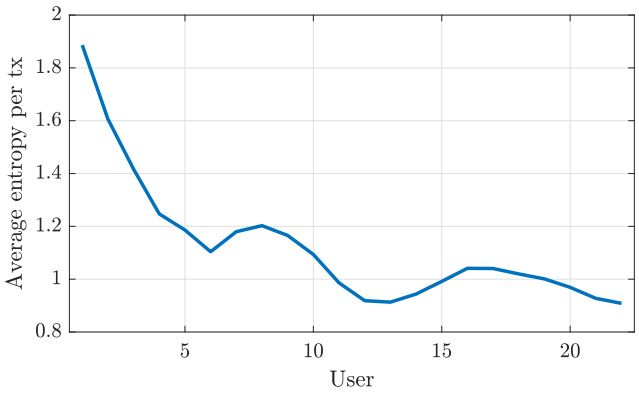

Fig. 4. Average entropy of the transmitters in the map versus the number of users who have contributed to the map in cooperative Channel-SLAM.

that the receivers are equipped with antenna arrays of nine elements arranged in a uniform 3×3 grid, such that both ToA and AoA information is available.

B. Evaluations and Discussion

As discussed above, transmitters with a high uncertainty do not provide much information regarding the user position and at the same time occupy a lot of memory. In addition, these transmitters may dilute the map matching performance. We exclude such transmitters from maps that are exchanged among users. In particular, we calculate the covariance matrix of the particles representing a transmitter's state. If the trace of this covariance matrix is above a heuristic threshold of $20\,\mathrm{m}^2$, the transmitter is excluded from the comprehensive map.

To evaluate the performance of cooperative Channel-SLAM, a reference user walks on a dedicated trajectory of length $311\,\mathrm{m}$ in the scenario in Fig. 2. Beforehand, the reference user receives a prior map to which a number of users have contributed in the cooperative Channel-SLAM scheme described in Section II-C. For comparison, the reference user also walks along the trajectory without a prior map, i.e, with single user Channel-SLAM. The positioning performances in terms of the mean absolute error (MAE) are presented in Fig. 3. The different curves correspond to the number of users who have contributed to the map that the reference user receives. The results in Fig. 3 and in all other figures in this section are averaged over 250 Monte-Carlo simulations.

It can be seen from Fig. 3, that the MAE in the single user case keeps increasing over time. Only in the region around $80\,\mathrm{m}$, the MAE decreases, since the user walks in a small loop and can benefit from loop closure. However, if prior knowledge in form of a transmitter map is available, the error is substantially smaller. When many users have contributed to the map, the error is even bounded in the long run. Only towards the end, where the reference user experiences an unfavorable geometrical dilution of precision (GDoP), the error increases slightly.

While we have published a similar result before in [12], we have not yet evaluated the evolution of the transmitter maps in cooperative Channel-SLAM. In particular, we are interested in the evolution of the information content of these maps and the single transmitters in the maps. Thus, Fig. 4 shows the average entropy of a transmitter in the map after each of the 22 users has contributed to the map by going through the scenario in Fig. 2 with cooperative Channel-SLAM.

Since the overall entropy of a transmitter map is additive w.r.t. the single transmitters, it depends on the single entropies of the transmitter state estimates in the map, and also on the number of transmitters. In cooperative Channel-SLAM, a map tends to contain more transmitters the more users have contributed to a map, since users go through the same scenario on different trajectories and observe different sets of transmitters. In addition, inaccurate map matching and false data association decisions tend to cause an increase of the transmitter entropies. On the one hand, these effects lead to an increase of the map entropy over time. On the other hand, the observations, i.e., measurements, of the users tend to decrease a transmitter's entropy in the map. In particular the entropies of transmitters with a favorable GDoP for multiple users will decrease over time.

In Fig. 4, the overall entropy of the map divided by the number of the transmitters in the map is plotted versus the number of users that have contributed to the map in cooperative Channel-SLAM. Thus, it is the average entropy of a transmitter in the map after a number of users have contributed to the map. The entropy of each transmitter is approximated by Eq. (17) with the sigma points in Eq. (15) for $\kappa = 0$. We observe that the average entropy per transmitter decreases over time, especially in the beginning. Thus, the effect of the decreasing entropy of some transmitters in the map is stronger than the increase of entropy in the map due to new transmitters that are added to the map. However, at some points the average entropy increases, for example if a user goes along a track where they detect many new transmitters that are not yet in the map.

Transmitters with a high entropy do not provide the user with much information regarding the user location. Instead, the lower the entropy of a transmitter, the more beneficial it is for positioning. We are therefore not only interested in the

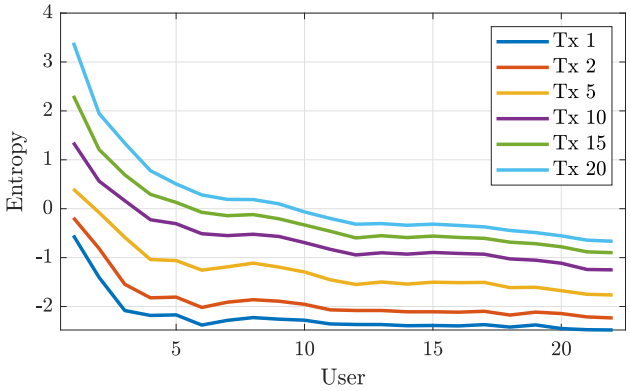

Fig. 5. Entropies of transmitters with least entropy in a map versus the number of users who have contributed to the map in cooperative Channel-SLAM. For example, the dark blue curve denotes the entropy of the transmitter with lowest entropy in the respective map.

average entropy of a transmitter map, but also in the entropies of the best transmitters in the map, i.e., the transmitters with lowest entropy.

Fig. 5 presents the entropies of such best transmitters in the map versus the number of users that have contributed to the map. For example, the dark blue curve denotes the entropy of the transmitter with lowest entropy in the map, and the red curve the entropy of the transmitter with second-lowest entropy in the respective map. We see that the best transmitter has converged after only six users that have contributed to the map. The entropy curves of the other plotted transmitters flatten out very much at that point.

V. Conclusion

We have shown before that the positioning error of cooperative Channel-SLAM is bounded in the long run outperforming single user Channel-SLAM. Within this paper, we have derived an approximation for the entropy of a transmitter state PDF when it is represented as a Gaussian mixture model. Analyzing the evolution of the entropies of transmitters in a comprehensive map, we have shown that not only the positioning error, but also the shared transmitter maps in cooperative Channel-SLAM converge quickly. Although there are constantly new transmitters added to the map, the average transmitter entropy in a map tends to shrink over time. In particular, the transmitters with lowest entropy converge already after only few users have contributed.

Based on these results, we can establish the relevance of transmitters in a map. In future work, we may analyze the tradeoff between the size of a map, i.e., the number of transmitters in the map, and the representation of these transmitters in the map on the one hand, and the positioning performance on the other hand. The communication load for exchanging maps may be decreased crucially if only relevant transmitter states are shared.

Acknowledgement

This work was partially supported by the DLR project Navigation 4.0.

References

[1] K. Yu, I. Sharp, and Y. J. Guo, *Ground-Based Wireless Positioning*. Wiley-IEEE Press, 2009.

[2] P. Meissner, C. Steiner, and K. Witrisal, "UWB Positioning with Virtual Anchors and Floor Plan Information," in *7th Workshop on Positioning Navigation and Communication (WPNC)*, Mar. 2010, pp. 150–156.

[3] A. O'Connor, P. Setlur, and N. Devroye, "Single-Sensor RF Emitter Localization Based on Multipath Exploitation," *IEEE Trans. Aerosp. Electron. Syst.*, vol. 51, no. 3, pp. 1635–1651, Jul. 2015.

[4] E. Leitinger, M. Fröhle, P. Meissner, and K. Witrisal, "Multipath-Assisted Maximum-Likelihood Indoor Positioning Using UWB Signals," in *IEEE International Conference on Communications Workshops (ICC Workshops 2014)*, Jun. 2014, pp. 170–175.

[5] K. Witrisal, P. Meissner, E. Leitinger, Y. Shen, C. Gustafson, F. Tufvesson, K. Haneda, D. Dardari, A. F. Molisch, A. Conti, and M. Z. Win, "High-Accuracy Localization for Assisted Living - 5G Systems will turn Multipath Channels from Foe to Friend," *IEEE Signal Process. Mag.*, vol. 33, no. 2, pp. 59–70, Mar. 2016.

[6] H. Wymeersch, N. Garcia, H. Kim, G. Seco-Granados, S. Kim, F. Wen, and M. Fröhle, "5G mm Wave Downlink Vehicular Positioning," in *IEEE Global Communications Conference (GLOBECOM)*, Dec. 2018, pp. 206–212.

[7] A. Shahmansoori, G. E. Garcia, G. Destino, G. Seco-Granados, and H. Wymeersch, "Position and Orientation Estimation Through Millimeter-Wave MIMO in 5G Systems," *IEEE Trans. Wireless Commun.*, vol. 17, no. 3, pp. 1822–1835, 2018.

[8] R. Mendrzik, F. Meyer, G. Bauch, and M. Win, "Localization, Mapping, and Synchronization in 5G Millimeter Wave Massive MIMO Systems," in *2019 IEEE 20th International Workshop on Signal Processing Advances in Wireless Communications (SPAWC)*, 2019, pp. 1–5.

[9] C. Gentner, T. Jost, W. Wang, S. Zhang, A. Dammann, and U.-C. Fiebig, "Multipath Assisted Positioning with Simultaneous Localization and Mapping," *IEEE Trans. Wireless Commun.*, vol. 15, no. 9, pp. 6104–6117, Sep. 2016.

[10] M. Ulmschneider, S. Zhang, C. Gentner, and A. Dammann, "Multipath Assisted Positioning With Transmitter Visibility Information," *IEEE Access*, vol. 8, pp. 155 210–155 223, 2020.

[11] M. Ulmschneider, "Cooperative Multipath Assisted Positioning," Ph.D. dissertation, Hamburg University of Technology, 2021.

[12] M. Ulmschneider, C. Gentner, and A. Dammann, "Cooperative Estimation of Maps of Physical and Virtual Radio Transmitters," in *Proceedings of 34th International Technical Meeting of the Satellite Division of the Institute of Navigation (ION GNSS+ 2021)*, Sep. 2021.

[13] T. Jost, W. Wang, U. Fiebig, and F. Perez-Fontan, "Detection and Tracking of Mobile Propagation Channel Paths," *IEEE Trans. Antennas Propag.*, vol. 60, no. 10, pp. 4875–4883, Oct. 2012.

[14] B. Fleury, M. Tschudin, R. Heddergott, D. Dahlhaus, and K. Pedersen, "Channel Parameter Estimation in Mobile Radio Environments Using the SAGE Algorithm," *IEEE J. Sel. Areas Commun.*, vol. 17, no. 3, pp. 434–450, Mar. 1999.

[15] M. Ulmschneider and C. Gentner, "RANSAC for Exchanging Maps in Multipath Assisted Positioning," in *IEEE International Conference on Industrial Cyber Physical Systems (ICPS)*, 2019.

[16] B. Anderson and J. Moore, *Optimal Filtering*, ser. Dover Books on Electrical Engineering. Dover Publications, 2012.

[17] J. A. Fessler and A. O. Hero, "Space-Alternating Generalized Expectation-Maximization Algorithm," *IEEE Trans. Signal Process.*, vol. 42, pp. 2664–2677, 1994.

[18] G. Celeux, S. Frühwirth-Schnatter, and C. Robert, "Model Selection for Mixture Models-Perspectives and Strategies," in *Handbook of Mixture Analysis*. CRC Press, Dec. 2018.

[19] S. Kaiser, M. G. Puyol, and P. Robertson, "Measuring the Uncertainty of Probabilistic Maps Representing Human Motion for Indoor Navigation," *Mobile Information Systems*, vol. 2016, pp. 9 595 306:1–9 595 306:15, 2016.

[20] T. M. Cover and J. A. Thomas, *Elements of Information Theory*, ser. Wiley Series in Telecommunications and Signal Processing. New York, NY, USA: Wiley-Interscience, 2006.

[21] J. K. Uhlmann, *Dynamic Map Building and Localization: New Theoretical Foundations*. University of Oxford, 1995.

[22] S. J. Julier, J. K. Uhlmann, and H. F. Durrant-Whyte, "A New Approach for Filtering Nonlinear Systems," in *Proceedings of the American Control Conference*, vol. 3, Jun. 1995, pp. 1628–1632.